AD-A148 801 CARS TEMPERATURE MEASUREMENTS IN SOOTING LAMINAR DIFFUSION FLAMES(U) UNITED TECHNOLOGIES RESEARCH CENTER EAST HARTFORD CT L R BOEDEKER ET AL. 30 JUL 84 TR-1 1/1

UNCLASSIFIED N00014-81-C-0046 F/G 20/13 NL

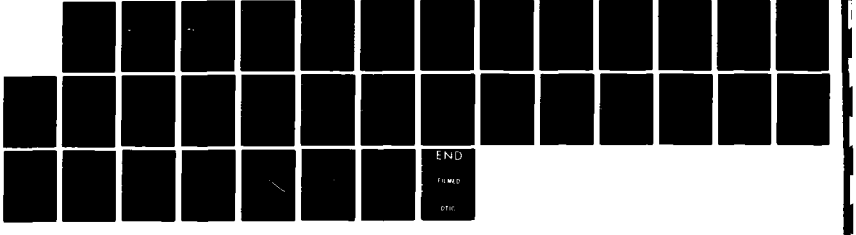

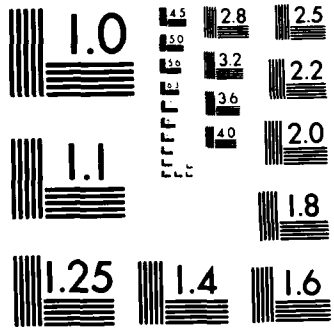

MICROCOPY RESOLUTION TEST CHART
NATIONAL BUREAU OF STANDARDS-1963-A

(12)

Technical Report No. 1
Contract N00014-81-C-0046; NR 094-411

AD-A148 801

CARS TEMPERATURE MEASUREMENTS IN SOOTING, LAMINAR DIFFUSION FLAMES

UNITED TECHNOLOGIES RESEARCH CENTER
East Hartford, Connecticut 06108

1 November 1984

Progress Report for Period 1 January 1981-
30 July 1984

Prepared for
OFFICE OF NAVAL RESEARCH
800 N. Quincy St
Arlington VA 22217

Technical Report No. 1
Contract N00014-81-C-0046; NR 094-411

CARS TEMPERATURE MEASUREMENTS IN SOOTING, LAMINAR DIFFUSION FLAMES

Laurence R. Boedeker
Gregory M. Dobbs

UNITED TECHNOLOGIES RESEARCH CENTER
East Hartford, Connecticut 06108

1 November 1984

Progress Report for Period 1 January 1981-
30 July 1984

Prepared for
OFFICE OF NAVAL RESEARCH
800 N. Quincy St
Arlington VA 22217

UNCLASSIFIED
SECURITY CLASSIFICATION OF THIS PAGE

AD-A148802

REPORT DOCUMENTATION PAGE

1a. REPORT SECURITY CLASSIFICATION: Unclassified	1b. RESTRICTIVE MARKINGS
2a. SECURITY CLASSIFICATION AUTHORITY	3. DISTRIBUTION/AVAILABILITY OF REPORT: Unlimited
2b. DECLASSIFICATION/DOWNGRADING SCHEDULE	
4. PERFORMING ORGANIZATION REPORT NUMBER(S): Technical Report 1	5. MONITORING ORGANIZATION REPORT NUMBER(S): Technical Report 1
6a. NAME OF PERFORMING ORGANIZATION: United Technologies Corp. Research Center; 6b. OFFICE SYMBOL (If applicable)	7a. NAME OF MONITORING ORGANIZATION: Office of Naval Research
6c. ADDRESS (City, State and ZIP Code): Silver Lane, East Hartford, CT 06108	7b. ADDRESS (City, State and ZIP Code): 800 N. Quincy Street, Arlington, VA 22217
8a. NAME OF FUNDING/SPONSORING ORGANIZATION: Same as Block 7a.; 8b. OFFICE SYMBOL (If applicable)	9. PROCUREMENT INSTRUMENT IDENTIFICATION NUMBER: N0014-81-C-0046 NR094-411
8c. ADDRESS (City, State and ZIP Code): Same as Block 7b.	10. SOURCE OF FUNDING NOS. — PROGRAM ELEMENT NO. / PROJECT NO. / TASK NO. / WORK UNIT NO.
11. TITLE (Include Security Classification): CARS Temperature Measurements in Sooting, Laminar Diffusion Flames	
12. PERSONAL AUTHOR(S): Boedeker, L. R. and Dobbs, G. M.	
13a. TYPE OF REPORT: Progress Report; 13b. TIME COVERED: FROM 1/1/81 TO 7/30/84	14. DATE OF REPORT (Yr., Mo., Day): 84,11,1; 15. PAGE COUNT: 29
16. SUPPLEMENTARY NOTATION	
17. COSATI CODES — FIELD / GROUP / SUB. GR.	18. SUBJECT TERMS (Continue on reverse if necessary and identify by block number): Soot Formation, Diffusion Flames, Flame Structure, Temperatures in Diffusion Flames, CARS Temperature Measurement

19. ABSTRACT (Continue on reverse if necessary and identify by block number)

Temperature distributions have been measured in axisymmetric ethylene-air diffusion flames using high spatial resolution coherent anti-Stokes Raman spectroscopy. As ethylene flow increased and the flame approached a smoke-point condition, the temperatures attained in the upper part of the flame were reduced by about 300K below maximum radial temperatures low in the flame. Addition of diluent N_2 to ethylene caused a reduction in temperature low in the flame but increased temperature higher in the flame. Maximum temperatures attained in all ethylene flames were between 0.84 and 0.89 of respective adiabatic flame temperatures (AFT). The upper temperature of the near-smoke-point flame was only 0.76 of AFT. Results are compared with the generalized flame front model of Mitchell. MIE scattering measurements are also discussed. Brief studies with propane and a nonsooting, CO flame are reported; maximum axial and radial temperatures were between 0.84 and 0.87 of AFT. Results indicate the importance of thermal loss from soot

20. DISTRIBUTION/AVAILABILITY OF ABSTRACT: UNCLASSIFIED/UNLIMITED ☒ SAME AS RPT ☐ DTIC USERS ☐	21. ABSTRACT SECURITY CLASSIFICATION: Unclassified
22a. NAME OF RESPONSIBLE INDIVIDUAL	22b. TELEPHONE NUMBER (Include Area Code); 22c. OFFICE SYMBOL

DD FORM 1473, 83 APR — EDITION OF 1 JAN 73 IS OBSOLETE.

UNCLASSIFIED
SECURITY CLASSIFICATION OF THIS PAGE

/radiation, radial transport processes and fuel pyrolysis. Nonluminous radiation and finite reaction rates are other possible factors. The upper luminous part of the highly sooting ethylene flame is likely above the primary flame front and is a soot burnout zone. /

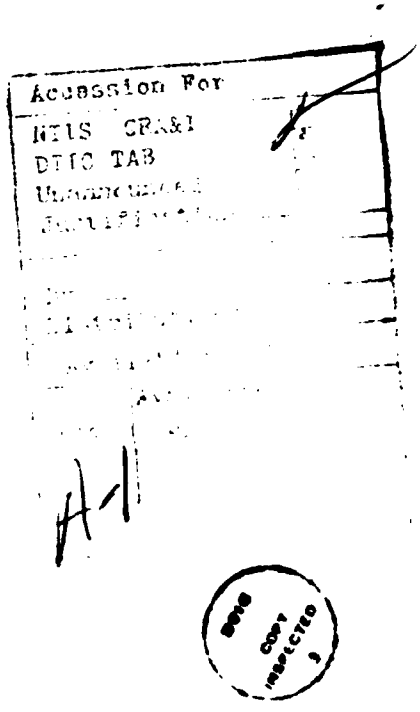

CARS TEMPERATURE MEASUREMENTS IN SOOTING, LAMINAR DIFFUSION FLAMES

Laurence R. Boedeker and Gregory M. Dobbs
United Technologies Research Center
East Hartford, CT. 06108

Abstract - Temperature distributions have been measured in axisymmetric ethylene-air diffusion flames using high spatial resolution coherent anti-Stokes Raman spectroscopy. As ethylene flow increased and the flame approached a smoke-point condition, the temperatures attained in the upper part of the flame were reduced by about 300K below maximum radial temperatures low in the flame. Addition of diluent N_2 to ethylene caused a reduction in temperature low in the flame but increased temperature higher in the flame. Maximum temperatures attained in all ethylene flames were between 0.84 and 0.89 of respective adiabatic flame temperatures (AFT). The upper temperature of the near-smoke-point flame was only 0.76 of AFT. Results are compared with the generalized flame front model of Mitchell. MIE scattering measurements are also discussed. Brief studies with propane and a nonsooting, CO flame are reported; maximum axial and radial temperatures were between 0.84 and 0.87 of AFT. Results indicate the importance of thermal loss from soot radiation, radial transport processes and fuel pyrolysis. Nonluminous radiation and finite reaction rates are other possible factors. The upper luminous part of the highly sooting ethylene flame is likely above the primary flame front and is a soot burnout zone.

INTRODUCTION

Temperature is an important controlling variable for soot formation in axisymmetric, laminar, diffusion flames. Glassman and Yacarino (1981), Sidebotham and Glassman (1983) and Gomez et al. (1984) have shown that the reciprocal of the fuel mass flow rate at the smoke height, when plotted against the reciprocal of the calculated adiabatic flame temperature (AFT) for nitrogen-diluted diffusion flames provides a convenient method for ranking the sooting tendency of fuels. We have been investigating soot formation and diffusion flame structure with the intent of providing internal flame temperatures and soot particle distributions aimed at understanding the physical and chemical basis of this correlation and the influence of fuel structure.

Temperature is difficult to measure in a sooting environment, and most prior studies have employed qualitative measurements using thermocouples. We report temperature measurements here using coherent anti-Stokes Raman spectroscopy (CARS). The measurements raise some questions about diffusion flame structure and the influence of soot particle radiation as an important heat loss. Some of the results are compared with simple generalized Burke-Schumann flame calculations performed using the model developed by Mitchell et al. (1980).

Ethylene was used as the fuel to examine highly sooting conditions while CO provided a soot free flame for comparison. Temperature distributions are reported for various amounts of fuel and diluent N_2. A brief investigation is also reported using propane, the fuel employed in a previous study by Eckbreth and Hall (1979). In general, these new studies show that peak temperatures are 200-400K lower than the adiabatic flame temperature (AFT) whereas the prior results showed peak values much closer to the AFT. Previously reported temperatures were high in fuel rich regions due to nonresonant susceptibility effects. We have shown recently (Hall and Boedeker, 1984) that these effects can be accounted for by introduction of a two parameter algorithm.

Soot particle distributions have been measured using MIE scattering. A few of these results will be discussed qualitatively here where they pertain to flame structure. The MIE results will be discussed more completely in a subsequent publication when CARS and MIE studies underway with other gaseous fuels are completed.

Santoro and Semerjian (1984) have studied soot formation in a similar ethylene-air diffusion flame. They used thermocouples for temperature and results presented here represent a contribution to needed comparisons under similar experimental conditions. Flower and Bowman (1984) and Farrow et al. (1984) at Sandia have been performing soot formation, CARS and thermocouple measurements in a two-dimensional ethylene-air diffuson flame. Excellent agreement was found in non-sooting and sooting regions between CARS data and their rapid-insertion thermocouple measurements. Their CARS results, while precise, are limited in scope. They were obtained with high spectral resolution, scanning CARS, and polarization suppression of the nonresonant background signal. Results reported here were obtained without suppressing the background and use of the two parameter model mentioned above. A broadband approach and somewhat less spectral resolution were employed. As a consequence it has been possible to reduce data acquisition time significantly and obtain an extensive set of CARS temperature data. Data accuracy, as discussed below, remained high enough to provide significant comparisons. Although not reported here, the second parameter provides valuable qualitative information on the location of the fuel zone and the onset of fuel pyrolysis, which will be useful in future considerations of detailed flame structure.

EXPERIMENT

Laminar, axisymmetric diffusion flames were studied using a 1.0 cm diam. burner, similar to the burner employed in the experiments of Glassman and colleagues. Air was supplied to an 86 cm^2 octagonal glass-walled duct surrounding the fuel tube. Glass beads and metal honeycomb were used to smooth the air flow. Fuels were of C.P. quality, used as supplied in gas cylinders. The flames were overventilated with typically a 2:1 velocity ratio between the air and fuel. Gas flows were monitored with mass flow meters and values recorded directly

into a PDP 11/34 computer which controlled operation of the experiment. Fuel and diluent mass flow meters were calibrated with a soap film technique. The airflow meter was calibrated with a positive displacement gas meter. Theoretical values of adiabatic flame temperature (AFT), for stoichiometric combustion of fuel and diluent with standard air, were calculated using the equilibrium computer code of Gordon and McBride (1976).

Spatially-precise, averaged, broadband nitrogen CARS spectra were recorded using folded-BOXCARS phase matching. Details of the CARS technique can be found in Hall and Eckbreth (1984). The sampling volume was approximately 0.7 mm long and 0.15 mm in diameter. The two pump beams at 532.0 nm and the approximately 120 cm^{-1} FWHM broadband Stokes beam entered the burner region through one of the flat glass window sections of the chimney. The position of the burner was adjusted with a stepping-motor driven positioning system with a positional resolution of 0.0127 mm. The CARS beam, near 473 nm, emerged from the burner spatially separated from the other laser beams and was optically collimated and focused into a holographic grating spectrograph. The dispersed CARS beam was detected with a 500 channel PAR optical multichannel analyzer (OMA 2). The OMA data and burner position were acquired by the PDP 11/34 computer. The experimental data files were later transferred to a VAX 11/750 for analysis.

Accuracy of the CARS temperature measurements is determined by the laser parameters, spectrometer conditions, averaging time, analysis uncertainties and interferences. A Quanta-Ray frequency-doubled Nd:YAG laser provided the two pump components. The pump laser line width was about 1.0 cm^{-1}, much larger than the N_2 Raman linewidths. The path length difference between the two pump components is about equal to the equivalent path length traveled by one beam in the beamsplitter used to provide the two beams, or about 1.6 cm. Hence, the two pump beams are likely uncorrelated, and laser field statistic effects that were noted by Rahn et al. (1984) should be unimportant here. The statistical character of our lasers is being investigated and will be reported at a later time. Spectral resolution varied from 1.1 to 1.4 cm^{-1} during the tests. Spectra were averaged over 500 laser shots (50 seconds at 10 Hz). Because the dye center frequency and bandwidth are very important input parameters in the analysis, particular care was exercised to ensure that these parameters were known as accurately as possible. CARS spectra of pure CO_2 or of ethylene with trace amounts of N_2 were taken before and after each spatial scan; these spectra were generated from the nonresonant background and thus provided a representation of the dye laser profile. The base lines of all experimental signatures were corrected for OMA dark current and flame radiation by subtracting the count levels obtained over the same averaging time when one of the two pump components was blocked. In sooting regions, a small C_2 (formed by laser vaporization of soot particles) Swan band radiation also contributes to the background count; this is primarily an incoherent effect generated by the simultaneous presence of the pump and Stokes sources and is corrected for by the above experimental procedure. The detailed nature of this interference was investigated by Eckbreth (1979). Analysis of experimental CARS spectra

was carried out with a two parameter, least-squares fitting routine. Details of this analysis for the present case can be found in Hall and Boedeker (1984). The spectra were analysed using the standard convolution given by Yuratich (1979). Teets (1984) has pointed out that when nonresonant background effects are present and the pump laser linewidth is much larger than the Raman linewidth of the probed molecule, a modified convolution should be employed. When the Yuratich convolution is employed in such cases Teets has shown that temperature results can be slightly high and concentrations somewhat low. On the fuel side of undiluted ethylene diffusion flames, we believe our temperature uncertainty is somewhat larger as a result. The measurements and flame-sheet model indicate that N_2 concentration builds up rapidly along the centerline of the undiluted flames studied, which helps to minimize uncertainty due to convolution. Our overall estimate of temperature uncertainty due to all the above considerations for the present experimental spectra is about +75/-125K in an undiluted ethylene fuel region and about +50/-50K for postflame conditions, in ethylene flames diluted with N_2, or for CO flames. The fitting codes are in the process of being altered to provide the modified convolution. A program of calibration tests with a reference observation furnace and known gas mixtures is in progress. It will also be possible to obtain a few CARS spectra in lower temperature regions of the fuel zone with polarization suppression in the near future. Hence improved temperature accuracy is anticipated in fuel rich zones for fuels with large nonresonant susceptibilities. This will be of importance for correlation of temperature and soot measurements and for detailed flame structure interpretations. However, data accuracy has been sufficient for present considerations. Finally it should be noted that Eckbreth and Hall (1979) discuss how careful radiation corrected thermocouple and sodium line reversal measurements were made with premixed flat flames as an early check on CARS accuracy in high temperature, soot-free, post-flame regions. Agreement of thermocouple results with CARS was obtained within 40K over a 1600-2100K temperature range.

Soot properties are measured using angular dyssymmetry MIE scattering and extinction. One of the pulsed, 532.0 nm CARS pump laser is highly attenuated and used for these measurements. The pump beam duration is about 10 ns and the repetition rate is 10 Hz. Scattered light is detected with photomultipliers and measured with a BOXCAR averager. Relative scattering at 90 degrees is reported here to infer the location of the soot zone inside the zone of flame luminosity. Detailed MIE measurements and soot properties will be reported in a later publication.

RESULTS

Measurements with propane

Temperature distributions in a propane-air diffusion flame were reported by Eckbreth and Hall (1979) as an early demonstration of the application of the CARS technique in a highly sooting environment. The CARS spectra were analyzed at that time with a constant nonresonant background and visual matching

of experimental and computer generated spectra. As mentioned above, the present spectra are acquired directly by the computer and are analyzed with a two parameter least-squares fitting technique. Recent work by Hall and Boedeker (1984) in an ethylene-air diffusion flame has shown that nonresonant susceptibility of hydrocarbon fuels can affect the analysis of experimental spectra in fuel-rich regions well beyond the lip of the burner and essentially throughout the region inside the flame front. The extent of the effect was not clearly evident in the Eckbreth and Hall work.

Recently we have made some measurements in a similar propane-air diffusion flame with our burner. The height of our flame was set to match the Eckbreth-Hall flame, about 30 mm, by adjusting the fuel flow rate and observing the luminous tip with a cathetometer. Our results are compared with the Eckbreth and Hall values for axial temperature distribution in Figure 1. The Eckbreth and Hall results indicated that peak axial temperature reached about 2200K just below the luminous tip, very close to the AFT of 2268K. Radial temperature results reported by them indicated off-axis temperature reached the AFT. Our results shown in Figure 1 indicate that peak axial temperature is only about 1900K, almost 400K below the AFT. Our radial results show a peak off axis temperature of about 1950K. This difference in peak temperature results in propane can be explained by the nonresonant susceptability effects that could be included in the analysis of our data. It was possible to digitize one or two of the 1978 photographs from the Eckbreth and Hall data set obtained inside the luminous zone. These spectra were analyzed with the present two-parameter fitting code and temperatures were reduced by 200 or 300K. Analysis of present data with only a one parameter fitting code would increase values inside the luminous zone by 200 or 300K. The values of temperature above the luminous zone for the two data sets shown in Figure 1 suggest that the two flames were not identical. As indicated in Figure 1 the two burners had slightly different dimensions and air flow geometries. The 1978 burner also employed some air flow swirl for flame stabilization. Hence, the two data sets are believed to show a consistant picture of the temperatures above the flame.

Experimental studies with ethylene

Studies of soot formation in diffusion flames have often included extensive results with ethylene (Glassman and Yaccarino, 1981). Present CARS measurements with ethylene have focussed on the roles of fuel flowrate and inert dilution in approaching a smoke-point condition as defined by Glassman and Yaccarino. At low fuel flow, a highly luminous, but non-smoking, ethylene flame was studied. At high fuel flow, a taller ethylene flame was investigated which was close to, but slightly below, the smoke height. This flame had clear visual evidence of the soot wings pictured by Glassman and Yaccarino. The effect of inert diluent on the near-smoke-point flame was investigated by adding progressively more amounts of nitrogen with the fuel flowrate held constant.

The ethylene flowrate for the shorter, undiluted flame was 1.4 std. cm^3/sec. Height of the luminous tip was 24 mm. Detailed temperature measurements were made in this flame to serve as a reference. Here, a summary of results is given. Several radial profiles were measured starting at 0.5 mm above the burner lip, the closest approach to the fuel tube without clipping the Stokes or CARS beams. These radial profiles were complemented by an axial profile along the flame centerline. In scanning from the flame centerline out through the soot zone, flame front and then into the cool surrounding air, typically 20 data points were acquired with a spatial step size as small as 0.3 mm. The total number of data points acquired was about 180. These points were used as the input to a computer program which generated a temperature contour map of the flame, shown here in Figure 2. Maximum radial temperature increased rapidly above the burner, attaining a level of 2000K at a height of about 4 mm. This value occured at a radius of 5 mm. Above this height the contours in Figure 2 show a large plateau level of temperature between 1900 and 2000K was formed which spread towards the flame centerline and persisted until a height of about 19 mm. At the luminous tip of the flame, the temperature had dropped slightly to about 1800K. The maximum temperature, 2000K is about 84% of the AFT, which for ethylene in air as given by Glassman and Yaccarino (1981) is about 2380K.

The height of the taller undiluted ethylene flame was measured and found to be 76 mm. This corresponded to a fuel flowrate of 3.4 std. cm^3/sec. Above this fuel flowrate, the height of the flame at the actual smoke point was 94 mm, in close agreement with the results of Glassman and Yaccarino (1981). Results for this 76 mm tall flame are presented in more detail here since they indicate that the temperature distribution undergoes a change at high fuel flowrate relative to the zone of soot luminosity. Radial temperature scans again indicated that peak temperature increased rapidly with height above the burner. Radial temperature distributions are shown in Figure 3 for heights at and above the station at which maximum radial temperature occured. It can be seen that peak radial temperature of 2100K was attained at a height $z = 15$ mm. This level was detectably higher by about 100K than was observed anywhere in the shorter ethylene flame. The 2100K peak occured at a radius of about 5.5 mm. Photographs of the flame show that soot luminosity at $z = 15$ mm starts closer to the centerline at a radius $r = 4.5$ mm. The flame was also photographed through an available narrow bandpass filter (1.2 nm) centered at 430.7 nm, in the CH emission band. These photographs showed that blue emission near $z = 15$mm extended about 1 mm beyond the luminous soot emission, or about to the peak temperature location. This outer zone is expected to be the region of CO burnout (Mitchell et al., 1980). The flame bands of CO are known to contain a complex structure from 300 to 500 nm (Gaydon, 1974), due to emission from excited CO_2. These results indicate that the temperature peak measured at $z = 15$ mm is occuring at the expected location in this region of the flame (Mitchell et al., 1980). Further details on the reduction of CARS data for $z = 15$ mm, and at $z = 7.6$ and 3.8 mm in this flame are contained in Hall and Boedeker (1984).

A change in the temperature structure of the 76 mm high flame is indicated by the data contained in Figure 3 for heights z =25.4 and z = 38.0 mm. A relatively sharp drop in peak temperature is indicated, from 2100K at 25.4 mm to about 1850K at 38.0 mm. Note that z = 38.0 mm is only 50% of the overall luminous height of the flame. For the shorter ethylene flame discussed above this type of temperature change did not occur until about 19 mm, or about 80% of the luminous flame height. Two possibilities arise to explain these observations; either a change has occured in the flame structure based on only observations of soot luminosity or an additional loss mechanism has become significant to induce a reduction in flame temperature. An additional loss mechanism might be thermal radiation from the soot as suggested by the radiation loss measurements of Markstein and de Ris (1984). In order to explore these possibilities further, the 76 mm flame was modified by adding an inert diluent to the fuel, maintaining constant ethylene flowrate. The diluent was N_2, which was known from prior studies (Glassman and Yaccarino, 1981) to reduce the amount of soot formed in the flame. The radial profiles were repeated at z = 15.0 and 38.0 mm.

At z = 15 mm N_2 was added in molar ratios of 1.0 and 3.0 relative to the fuel, reducing the AFT to 2316 and 2187K respectively. Radial temperature profile results are shown in Figure 4. As would be expected, it can be seen that temperature is reduced with increasing diluent. Peak temperature remained at a relatively constant fraction of the respective AFT, however. With no diluent the peak temperature is about 88% of the AFT. For nitrogen/fuel of 1.0 and 3.0 the peak temperatures are about 86% of respective AFT's. Closer to the centerline, in the fuel zone, the temperatures in Figure 4 are seen to fall off faster than the AFT. Fuel pyrolysis and flame structure effects may explain this fall off. Essentially these diluent results at z = 15mm are about as expected.

The effect of inert diluent at z = 38.0 mm, however was not the same as at z = 15 mm. Here the effect has been investigated for nitrogen/fuel = 1.0. The radial profiles are shown in Figure 5. Somewhat suprisingly, addition of N_2 to the fuel has caused an increase in peak temperature of about 100K, a detectable change. The results in the important peak region were checked by performing a subsequent scan over several spatial points around the maximum temperature location for the diluted flame, then immediately repeating these spatial locations for the undiluted flame. Results confirmed the initial measurements as shown in Figure 5. It should be noted here that these peak radial temperatures occur in a flame region where the CARS convolution question discussed earlier is not a factor.

In order to explain the increase of temperature at z = 38 mm when nitrogen diluent was added, both flame structure and loss mechanisms must be considered. This is necessary because visual observation of the luminous tip showed an unexpected change. As noted the undiluted ethylene flame in this series was 76 mm in height. Addition of nitrogen in the molar ratio nitrogen/fuel = 1, for constant fuel flowrate, caused a reduction in height to 66 mm. Theoretical

considerations (Mitchell et al., 1980), however, would suggest that the flame should lengthen slightly as diluent is added. Further information on these considerations is provided by the axial temperature profiles that were obtained.

The axial temperature profiles obtained for an ethylene flowrate of 3.4 std. cm^3/sec are shown in Figure 6. Increasing amounts of nitrogen dilution were studied as shown, up to nitrogen/fuel molar ratio = 5.5. Low in the flame the effect of inert dilution is a reduction of temperature in the fuel pyrolysis zone, essentially an expected result. Higher in the flame, however, a crossover condition exists and the flames with nitrogen/fuel = 1.0, 3.0 achieve a higher absolute maximum temperature than the undiluted flame. Repeat data were obtained for the undiluted flame in the lower half. Repeatability was excellent, except near peak T. This may indicate a sensitivity to detailed flow conditions, since in general the undiluted flame profile seems to be very flat, reaching a fairly low maximum temperature earlier than would be expected. The maximum axial temperature results are summarized in Table 1. Nitrogen dilution is seen to have increased maximum temperature on a relative basis from 76% to 89% of respective adiabatic flame temperature. Such an increase is strongly suggestive of an additional loss process from the highly sooting undiluted flame, likely thermal radiation from the soot. If the undiluted flame had achieved 89% of its AFT then its maximum axial temperature would have been higher by about 300K. Note that low in this undiluted flame, at z = 15 mm, peak radial temperature did attain 2100K. Uncertainty in CARS data analysis due to the convolution question discussed earlier would only enhance the reduction of peak axial temperature in the undiluted flame relative to the diluted flames.

The location of the luminous tips is indicated on Figure 6. As mentioned previously, nitrogen dilution was observed to shorten the luminous zone. At the highest dilution ratio, 5.5, it was necessary to reduce the air flow to an underventilated condition in order to stabilize the flame. This underventilation is believed to have caused the flame to change shape and lengthen. A blue tip could be observed above the weak soot emission zone for this highest dilution. The length of this blue tip is indicated by the horizontal line attached to the tip arrow. All lower dilutions were achieved with about a 2:1 velocity overventilation of the air flow, and soot luminosity was high enough to preclude any direct observations above the luminous tip. Some photographs of these lower dilution ratio flames were made however, using the blue narrowband filter. The results for nitrogen/fuel = 1.0 are particularly interesting. Low in the flame they show that the blue zone extends radially out beyond the edge of the soot luminosity, as noted previously for the undiluted flame. Higher in the flame this outer blue emission zone disappears and only the blue tail of the soot luminosity remains. The tip region outline is virtually identical in the filtered and unfiltered photos. This suggests that the relative extents of the soot and flame reaction zones may have changed as dilution ratio increased from 1.0 to 5.5.

Further information about the axial structure of these ethylene flames was obtained by locating the soot zone using measurements of MIE scattering at 90 degrees. Results are shown in Figure 7 for dilution ratios of 0, 1.0, 3.0. Normalized scattering profiles are shown which indicate that the soot zone narrows sharply with increasing dilution. Maximum soot scattering occurs at the same location for each case. The amount of soot is reduced sharply with increasing dilution, as noted in the caption for Figure 7 by the relative scattering values that were measured at the peak location. Soot scattering was below the level of detectability for a dilution ratio of 5.5, but would occur within a narrow zone just below the luminous tip location given in Figure 6. These scattering measurements will be discussed further when some flame model results are presented later in this paper.

Nonluminous flame results with CO

The CARS temperature measurements in ethylene-air discussed above raise questions about structure of a sooting flame and energy loss due to thermal radiation from soot. These questions do not appear to be simple to address in a diffusion flame. A flame without soot luminosity, i.e. a nonluminous flame, would be a valuable reference point. Since CO is known to be non-sooting, even with hydrogen present, some CARS measurements were performed in a CO-air diffusion flame with our burner. Small amounts of hydrogen were added to the CO to provide flame stability. The nonresonant susceptability of CO is not a significant factor in the regions of the flames investigated since it is comparible to that of N_2.

Radial temperature profiles for an undiluted case are shown in Figure 8. The flowrate of CO was chosen to give a tall flame based on the gas phase emission profile observed. In general this emission was bluish-white up to about the middle of the flame and then a transition took place to a darker color tip region. The tip here occured at about 75 mm. The two radial profiles shown in Figure 8 were taken at approximately 30 and 50% of this tip height. The higher radial temperature profile is seen to have a broad peak near the axis of the flame. The lower profile peaks at a radius of about 4.5 mm. Maximum radial temperature attained at both heights is about 2060K, or about 87% of the adiabatic flame temperature.

Axial temperature profiles for the undiluted and a nitrogen-diluted case are shown in Figure 9. The profiles peak below the AFT values and the diluted profile peak occurs slighty higher above the burner. The maximum axial temperature of the undiluted CO flame was 2080K, essentially the same as maximum radial temperature. This axial peak occured at about 40 mm above the burner where radial results show an on-axis peak. Thus the darker colored tip appears to be above the primary flame reaction zone. The diluted CO flame attained a peak temperature of 1910K (84% of AFT) at about 45 mm. Hence the crossover observed with the ethylene flame is not present here. In addition an undiluted CO flame was tested with flowrate reduced from 945 to about 600 sccm. Peak (Peak) axial temperature was 2090K, and occurred at about 30 mm, hence heat

loss to the burner does not seem to be a significant factor here for the taller undiluted CO flame.

These results with CO certainly suggest that thermal radiation from soot may not be the only significant energy loss from a sooting flame. Nonluminous emission from CO_2 and H_2O may contribute to a noticeable reduction in flame temperature. Recent measurements and interpretation of radiative loss from a turbulent methane diffusion flame by Jeng et al. (1983) indicate that such gas phase radiative losses may be significant. Effects due to finite reaction rate chemistry of CO burnout may also influence temperature. Slow rates and the possibility of nonequilibrium radical concentrations in CO flames were recognized some time ago, as summarized by Gaydon (1974). Heat conduction losses to the air outside the stoichiometric air layer need to be considered, however.

Results with generalized Burke-Schumann model, comparison with experiment

Calculations were performed with a nonradiative model which accounts for transport properties and natural convection (Mitchell et al. 1980). Mitchell's model is a flame sheet model which does not account for multiple step, finite reaction rate chemistry. The model also does not account for pyrolysis of the fuel due to radial heat conduction from the flame into the fuel rich zone. Radial transport properties of all remaining species are modeled however, hence heat loss by radial transport to the air mass outside the stoichiometric air layer is part of the model. Heats of reaction are balanced by convective and molecular transport processes to determine the temperature field.

The output from the model includes species concentration profiles, radial and axial velocity distributions, and temperature distributions. Results for temperature distribution are reported here for comparison with experimental results. Several ethylene cases have been studied at this time. Radial temperature distribution results are summarized in Figure 10, and axial profiles are shown in Figure 11.

Radial calculations correspond closely to the heights, fuel flow and nitrogen dilution conditions shown in the experimental results of Figures 4 and 5. For both lowest and highest heights, Figures 10a and 10b, nitrogen dilution causes a reduction in temperature. The experimental results of Figure 5 show a crossover condition at the higher location when N_2 was added. Quantitatively the model is predicting substantially lower peak temperatures at the lower height, Figure 10a than were measured, Figure 4. Higher in the flame predicted, Figure 10b and measured, Figure 5 peak radial temperatures are closer quantitatively; however as noted the effects of N_2 addition are reversed. The radial resolution grid used in the model is seen to resolve the calculated temperature peak profile very well. The calculated flame front is slightly outside the burner tube lower in the flame and is slightly inside the burner at the higher location, results that are in agreement with the measurements. Calculated peaks are much sharper than measured profiles, particularly lower in the flame, which indicates that finite reaction rates are important. Note that peak cal-

culated temperature lower in the flame, Figure 10a seems to scale very well with AFT, while close to the center line these radial profiles show a much stronger effect of N_2 on reducing temperature levels. These trends are exactly what was observed in the measurements, Figure 4.

The calculated axial temperature results shown in Figure 11 correspond to the same ethylene flowrate and nitrogen dilutions as the experimental results, Figure 6. Calculated axial temperature profiles are well resolved by the grid and are seen to reach peak levels below the AFT values, attaining for each dilution about 0.83 of AFT. This result indicates that the model is predicting significant loss by radial transport to the air that was outside the stoichiometric layer at the start of the flame. In preliminary calculations with coarse axial and radial grids, the flames all reached their respective AFT's, and flame lengths were just slightly shorter. Quantitatively, predicted peak axial temperature for the undiluted flame is now only about 150K higher than what was measured, while for the N_2/fuel = 3.0 case predicted temperature is about 200K lower than experimental results. The model may be overestimating radial losses but a more detailed examination of radial temperature, species concentration and velocity radial profiles is required. Low in the flame measured axial temperatures are higher than predicted results. This indicates that preheating of the fuel by the burner tube, in a regenerative mode, may be significant. The temperature of the burner tube reached about 650K at its exit in the undiluted flames, as measured with fine thermocouples that were welded to the outside of the tube. Such regenerative heat feedback is not part of the model.

Calculated flame length is seen on Figure 11 to increase slightly with N_2 dilution, from about 47 mm for the undiluted flame to 51 mm at N_2/fuel = 3.0. Further dilution at the reduced air flow, the N_2/fuel = 5.5 case, is seen to lengthen the calculated flame to about 58 mm. For the N_2/fuel = 0, 1.0, 3.0 cases the discrepancy between the luminous tip heights in the measurements, Figure 6, and the calculated flame lengths, Figure 11, is seen to be reduced substantially with increasing dilution. When combined with the MIE scattering results of Figure 7, this comparison suggests that the luminous tip height of the undiluted flame is considerably above the true experimental end of the flame. Disappearance of soot is direct evidence for the existence of an oxidation zone. The MIE curves, Figure 7, narrow considerably with increasing dilution. They all peak, as noted previously, at the same height and the height at which the slope of the curve starts to decrease sharply does increase slightly with dilution. In this context the predicted and measured flame lengths are in excellent agreement. For the undiluted, near smoke-point flame then there is likely a large soot burnout zone at the top of the flame which is luminous and masks the true flame shape. Measurements of oxidant species concentrations, OH and O_2, are needed along the flame axis to confirm these suggestions. In addition the nonresonant susceptability needs to be measured directly inside the luminous zone to complement the second parameter data from the CARS measurements. Finally note that axial results with CO in Figure 9, while not modeled here, show clearly that N_2 dilution tends

to lengthen a flame. Also the shape of the CO flame tip as observed visually is not a good indication of the location of the flame front, indicating that in general visual characteristics need to be interpreted carefully.

If these flame length observations are correct then further discussion is possible about the meaning of the experimental radial temperature results obtained at z = 38 mm. This height would still be below the true end of the flame and hence high peak radial temperature might be expected. The fact that a larger than expected drop off in temperature was observed supports a soot radiative loss mechanism. However, at this time it is not possible to be sure about the soot free theoretical distribution of peak temperature along the flame front. Present experimental results certainly are not in agreement with the model. It may be important to incorporate fuel pyrolysis into the model to understand the flame temperature distribution results. The experimental temperatures measured on axis in the undiluted flame are high enough that substantial on-axis pyrolysis would be expected for these millisecond type dwell times quite low in the flame (Benson and Haugen, 1967). Thus a large part of the flame may in fact involve burning of an approximately equimolar mixture of acetylene and hydrogen, the primary products of ethylene pyrolysis (Benson and Haugen, 1967). The relative diffusion of these two species into a stoichiometric flame front would occur at different rates, probably consuming hydrogen faster than acetylene. At this time the primary experimental observations that support a soot radiative loss mechanism are the crossovers to higher temperatures that have been observed in both radial and axial results as the fuel was diluted with nitrogen and soot levels were reduced. Soot profiles have been measured radially and are being analyzed to provide soot size, number density and volume fraction information. Hence it will be possible to calculate soot radiative loss and check consistency of the soot and temperature fields.

CONCLUSIONS

The studies reported here have shown that the temperature attained in an ethylene-air diffusion flame near its smoke-point is reduced in the upper part of the flame by about 300K below the maximum radial temperatures measured low in the flame. This drop in temperature corresponds to a change from 0.89 to 0.76 adiabatic flame temperature (AFT) which appears to be occurring within the primary flame zone. Addition of diluent N_2 to ethylene caused a crossover to higher temperatures in both axial and radial results high in the flame. These results are likely explained by thermal radiation from the soot, in accord with the findings of Markstein and de Ris (1984) as well as others. In addition questions of flame structure relative to soot luminosity have been raised and partially answered. It is quite likely that the true flame height of the undiluted ethylene-air diffusion flame near its smoke-point is only about 60% of the height of the luminous zone. The measurements indicate that the generalized flame sheet model formulated by Mitchell et al. (1980) provides useful guidance in some areas such as flame length and axial temperature distribution early in the flame. The model suggests that radial thermal conduction and mass

transport can cause a significant reduction in peak axial temperature of the ethylene flame. Measurements with CO and diluted ethylene diffusion flames, which contain little or no soot, had maximum temperatures in the range of 0.84-0.89 of their AFT's. These maximum temperature results might be explained by radial transport losses, but other factors might be significant also, such as nonluminous gas radiation and finite reaction rate chemistry. Temperature profiles have much broader peaks compared to the model results which indicates that finite rate chemistry of CO burnout should be addressed. Measurements show that the AFT does appear to be a reasonable correlating parameter for maximum temperature in all the flames studies. Finally, fuel pyrolysis must be important but details are not clear in the temperature results at this time. Rapid pyrolysis and high conversion of ethylene to acetylene and hydrogen likely is occuring low in the undiluted ethylene flame. Perhaps this is a factor in the observed temperature distribution along the flame front for this case, since these pyrolysis products have significantly different diffusivities and hydrogen would be consumed faster than acetylene at the flame front. Certainly the model needs to be extended to a realistic treatment of pyrolysis in diffusion flames. The results of this study are expected to be of value in basic soot formation studies. The measurements are being extended to include other fuels and the structure of a diluted flame near its smoke-point.

ACKNOWLEDGEMENTS

This work was sponsored by the Office of Naval Research under Contract N00014-81-C-0046, NR 094-411 to UTRC and Princeton University. Discussions with and the early experimental work of Alan C. Eckbreth are gratefully acknowledged. Discussions with Profs. Glassman and Williams and other members of the Princeton University combustion groups are also gratefully acknowledged. The early experimental results of Allesandro Gomez were very helpful. Thanks are due to Dr. R. Mitchell of the Sandia Combustion Research Division for providing a copy of his diffusion flame model. Discussions with M. B. Colket have been very helpful. The valuable technical assistance of Edward J. Dzwonkowski is noted.

REFERENCES

Benson, S. W., and Haugen, G. R. (1967). Mechanisms for some high-temperature gas-phase reactions of ethylene, acetylene, and butadiene. J. Phys. Chem. 71, 1735.

Eckbreth, A. C. (1979). CARS investigations in flames. Seventeenth Symposium (International) on Combustion, 975.

Eckbreth, A. C., and Hall, R. J. (1979). CARS thermometry in a sooting flame. Combust. Flame, 36, 87.

Farrow, R. L., Lucht, R. P., Flower, W. L., and Palmer, R. E. (1984). Coherent anti-Stokes Raman spectroscopy measurements of temperature and acetylene spectra in a sooting diffusion flame. Twentieth Symposium (International) on Combustion, Abstract 140.

Flower, W. L., and Bowman, C. T. (1984). Measurements of the structure of sooting laminar diffusion flames at elevated pressures. Twentieth Symposium (International) on Combustion, Abstract 112.

Gaydon, A. G. (1974). The Carbon Monoxide Flame. In The Spectroscopy of Flames. John Wiley & Sons, New York, Chap. VI, pp. 127-142.

Glassman, I. and Yaccarino, P. (1981). The temperature effect in sooting diffusion flames. Eighteenth Symposium (International) on Combustion, 1175.

Gomez, A., Sidebotham, G., and Glassman, I. (1984). Sooting behavior in temperature-controlled laminar diffusion flames. Combust. Flame, 58, 45.

Gordon, S. and McBride, B. J. (1976). Computer program for calculation of complex chemical equilibrium compositions, rocket performance, incident and reflected shocks, and Chapman-Jouguet detonations. National Aeronautics and Space Administration, Report NASA SP-273.

Hall, R. J., and Boedeker, L. R. (1984). CARS thermometry in fuel-rich combustion zones. Appl. Opt., 23, 1340.

Hall, R. J., and Eckbreth, A. C. (1984). Coherent anti-Stokes Raman spectroscopy (CARS): application to combustion diagnostics. In Ready, J. F., and Erf, R. K. (Eds.), Laser Applications, Academic Press, New York, Vol. 5, pp. 213-309.

Jeng, S-M., Chen, L-D, and Faeth, G. M. (1983). The structure of bouyant methane and propane diffusion flames. Nineteenth Symposium (International) on Combustion, 349.

Jeng, S-M., Lai, M-C., and Faeth, G. M. (1983). Infrared radiation from gases in buoyant, turbulent methane diffusion flames. Chem. Phys. Processes Combust., Paper 34.

Mitchell, R. E., Sarofim, A. F., and Clomburg, L. A. (1980). Experimental and numerical investigation of confined laminar diffusion flames. Combust. Flame, 37, 227.

Rahn, L. A., Farrow, R. L., and Lucht, R. P. (1984). Effects of laser field statistics on coherent anti-Stokes Raman spectroscopy intensities. Opt. Lett., 9, 223.

Santoro, R. J., and Semerjian, H. G. (1984). Soot formation in diffusion flames: flow rate, fuel species and temperature effects. Twentieth Symposium (International) on Combustion, Abstract 108.

Sidebotham, G., and Glassman, I. (1983). Sooting behavior of cyclic hydrocarbons in laminar diffusion flames. Fall Technical Meeting, Eastern Section: The Combustion Institute, Paper 62.

Teets, R. E. (1984). Accurate convolutions of coherent anti-Stokes Raman spectra. Opt. Lett., 9, 226.

Yuratich, M. A. (1979). Effects of laser linewidth on coherent anti-Stokes Raman spectroscopy. Mol. Phys., 38, 625.

TABLE I

Effect of nitrogen dilution on maximum axial temperature attained in ethylene-air diffusion flames. Ethylene flowrate 3.4 std.cm^3/sec

N_2/Fuel Molar ratio	Maximum Axial Temperature	AFT	T_{max}/AFT
	K	K	
0	1820	2381	0.76
1.0	1900	2316	0.82
3.0	1940	2187	0.89
5.5	1730	2033	0.85

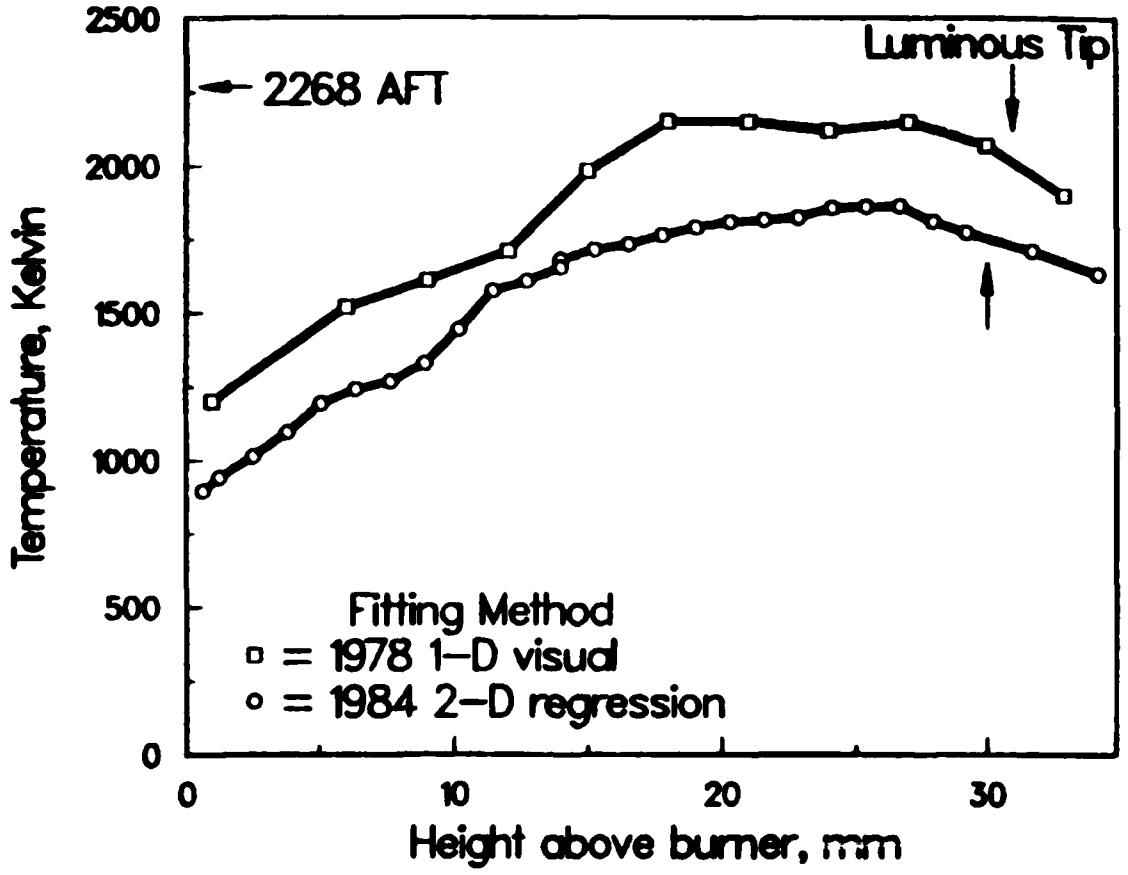

FIGURE 1 Propane diffusion flame axial temperature profile. Results compare 1978 and 1984 flames and methods. One dimensional visual fit was used in 1978 (□) by Eckbreth and Hall with 12.7 mm diam. fuel tube burner and 25 mm diameter swirled airflow. Two dimensional regression fit was used in present 1984 results (o) with 10 mm diam. fuel tube burner and unswirled 100 mm diameter glass walled airflow duct.

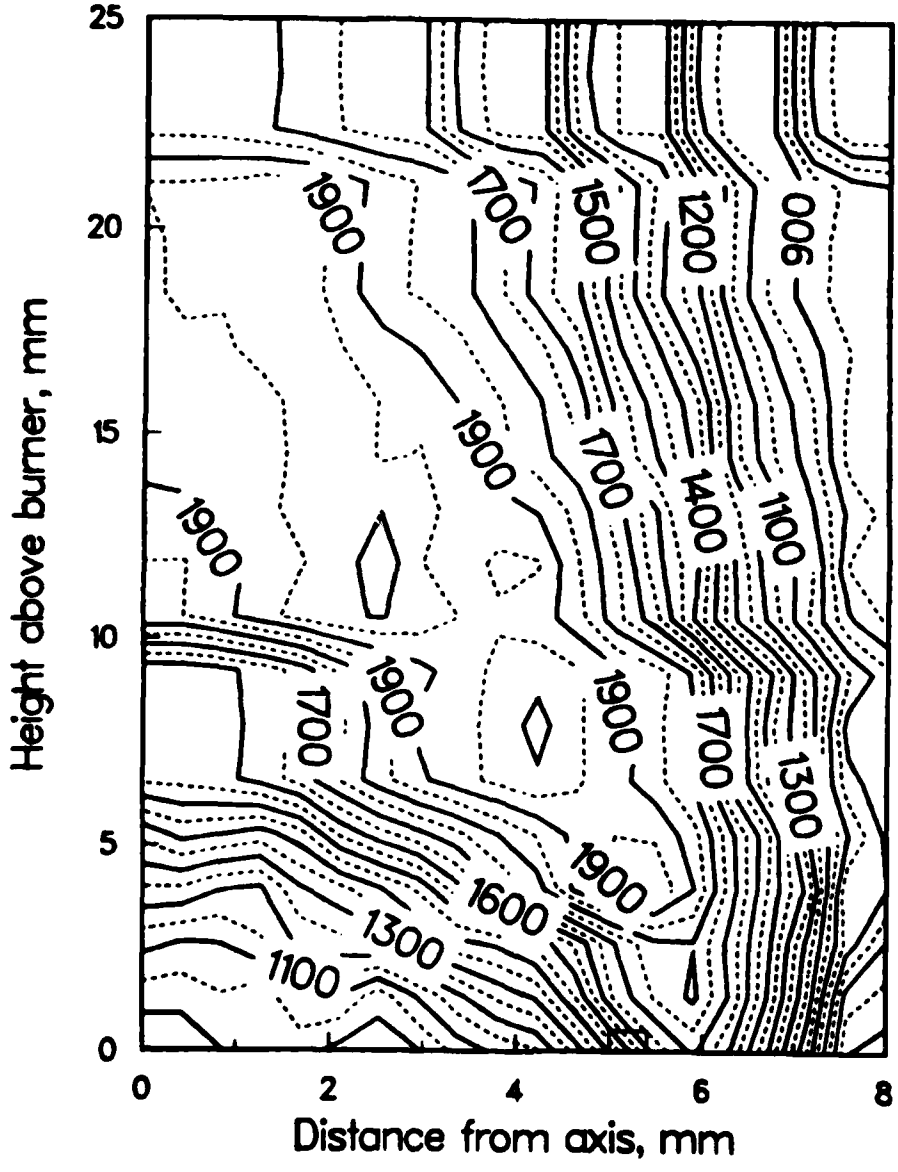

FIGURE 2 Computer generated contour map of temperature in Kelvin for 24 mm high undiluted ethylene-air diffusion flame. Ethylene flowrate $\dot{V}_f$ = 1.4 std. cm^3/sec. Approximately 180 data points in 8 radial and an axial scan were used to generate the contours.

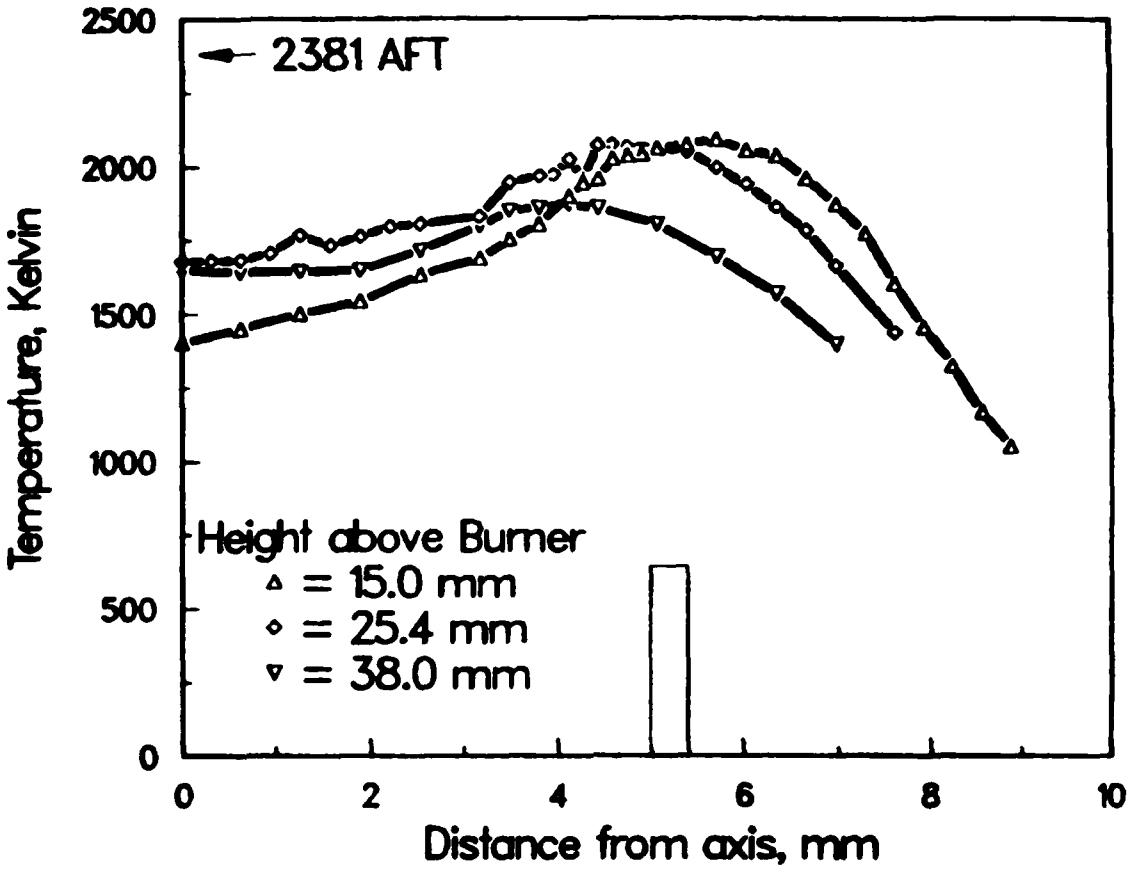

FIGURE 3 Radial temperature profiles for undiluted ethylene-air diffusion flame with fuel flowrate of $\dot{V}_f$ = 3.4 std. cm^3/sec and luminous height of h_f = 76 mm. Burner lip temperature is indicated by height of vertical bar. Width of bar indicates burner tube radial location and thickness. Adiabatic flame temperature (AFT) indicated on temperature scale.

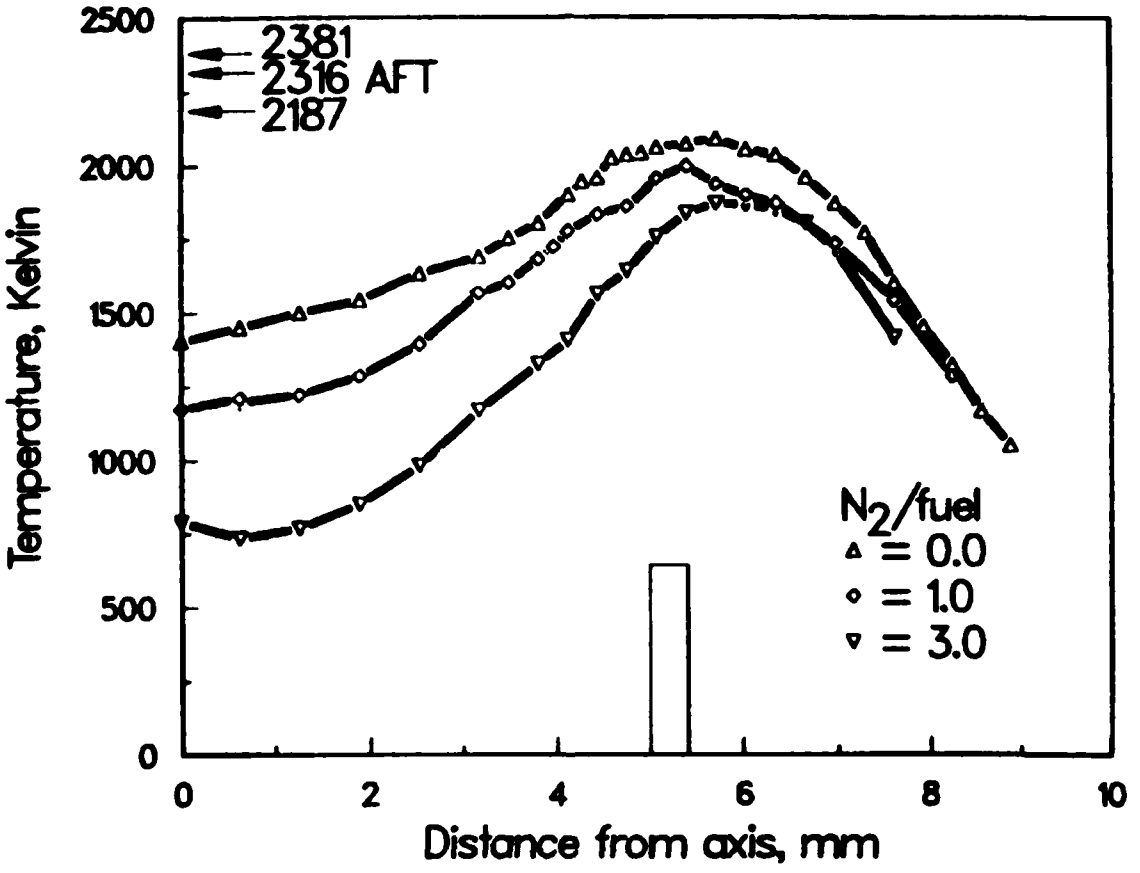

FIGURE 4 Effect of nitrogen dilution of fuel on radial temperature profiles 15 mm above burner. Ethylene flowrate 3.4 std. cm^3/sec. Burner lip temperature indicated by height of vertical bar for undiluted flame. Nitrogen dilution reduces theoretical adiabatic flame temperature as shown by AFT markers.

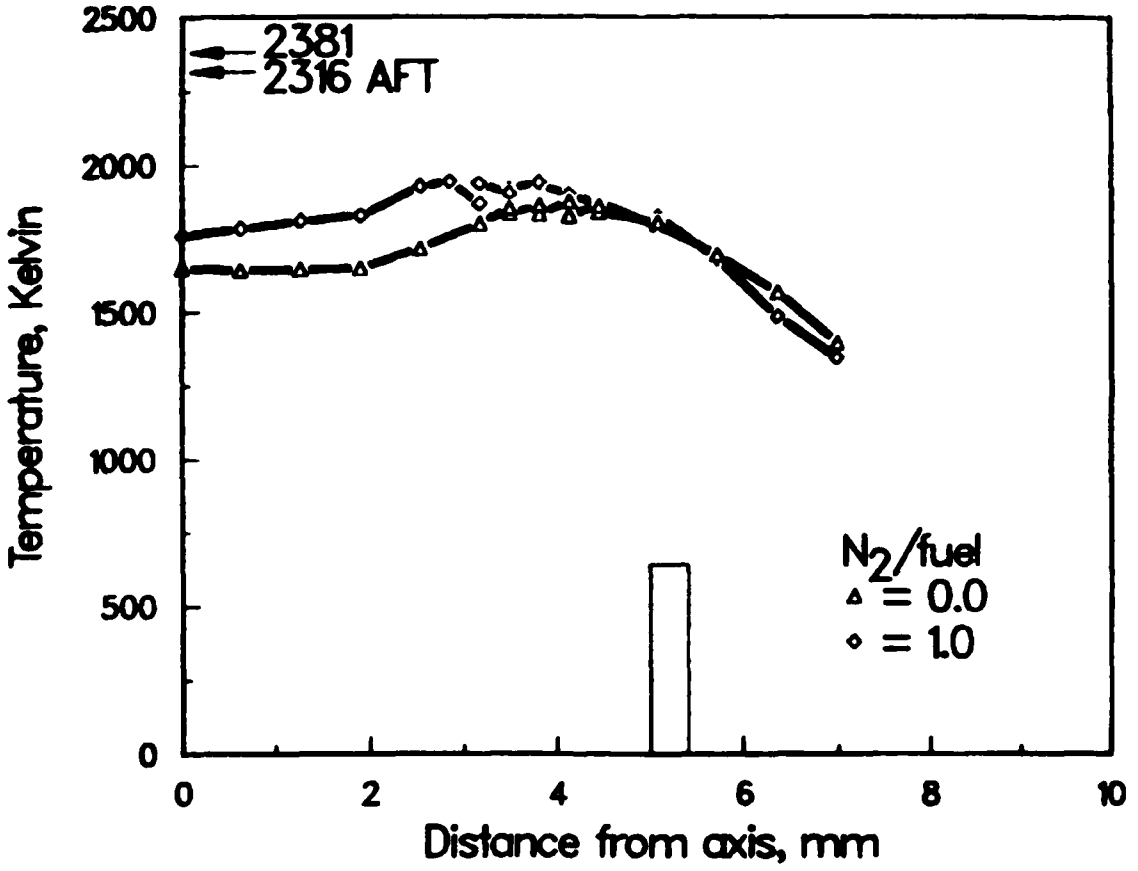

FIGURE 5 Effect of nitrogen dilution of fuel on radial temperature profile 38 mm above burner. Ethylene flowrate 3.4 std. cm^3/sec. Nitrogen dilution reduces theoretical adiabatic flame temperature as shown by AFT markers.

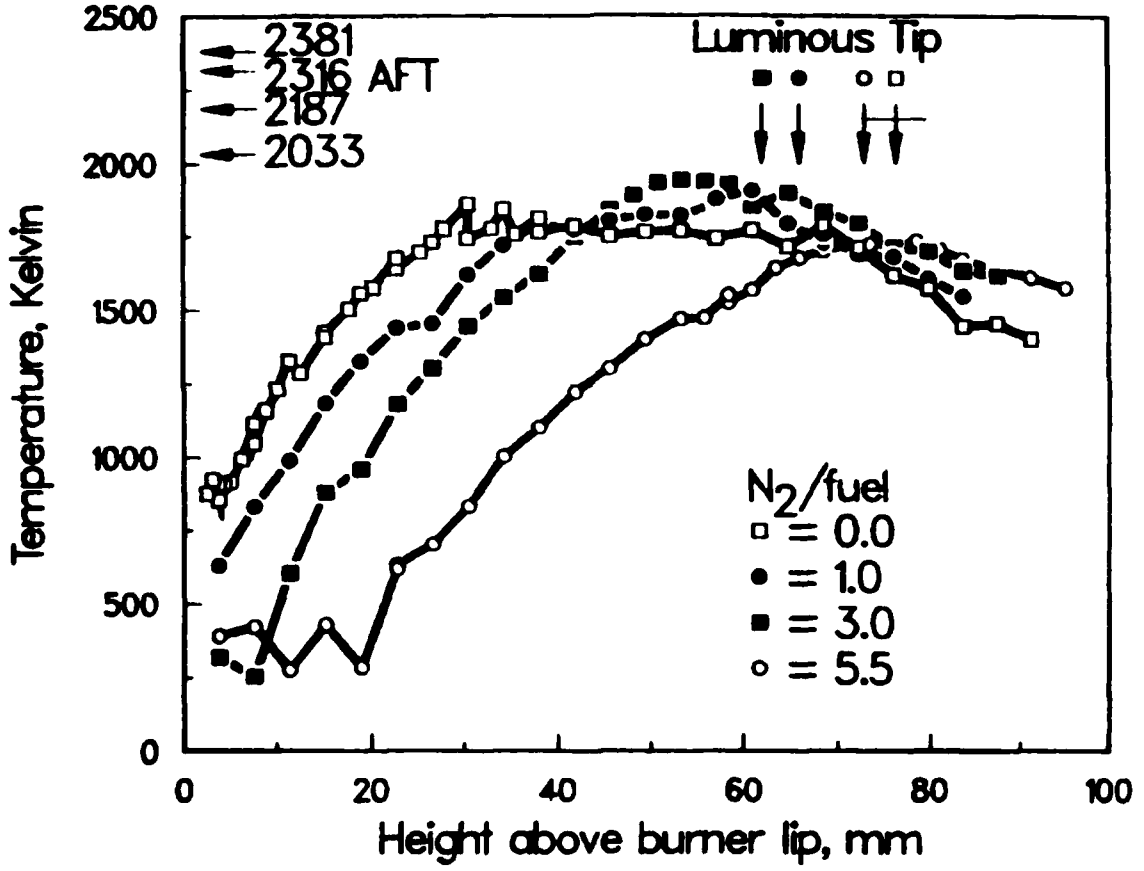

FIGURE 6 Axial temperature profiles for ethylene-air diffusion flame with ethylene flowrate 3.4 std. cm^3/sec. Profiles show effect of nitrogen dilution at constant fuel flowrate. Vertical arrows indicate height of luminous tip for dilution ratio indicated. Nitrogen dilution reduces theoretical adiabatic flame temperature as shown by horizontal AFT markers.

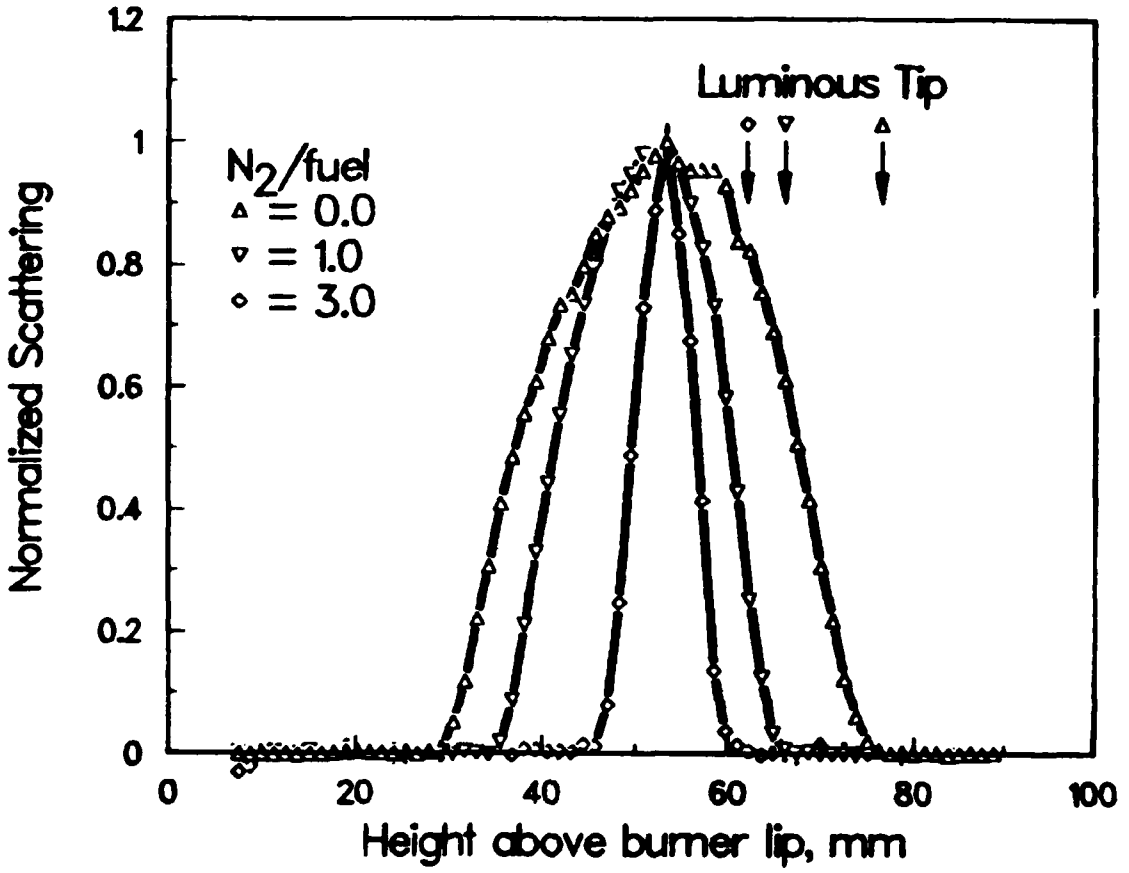

FIGURE 7 Normalized 90 degree MIE scattering profiles for ethylene flowrate of 3.4 std. cm^3/sec. Profiles show normalized effect of nitrogen dilution at constant fuel flowrate. Relative maximum scattering signals for N_2/fuel = 0, 1.0, 3.0 are 1.0, 0.34, 0.012 respectively.

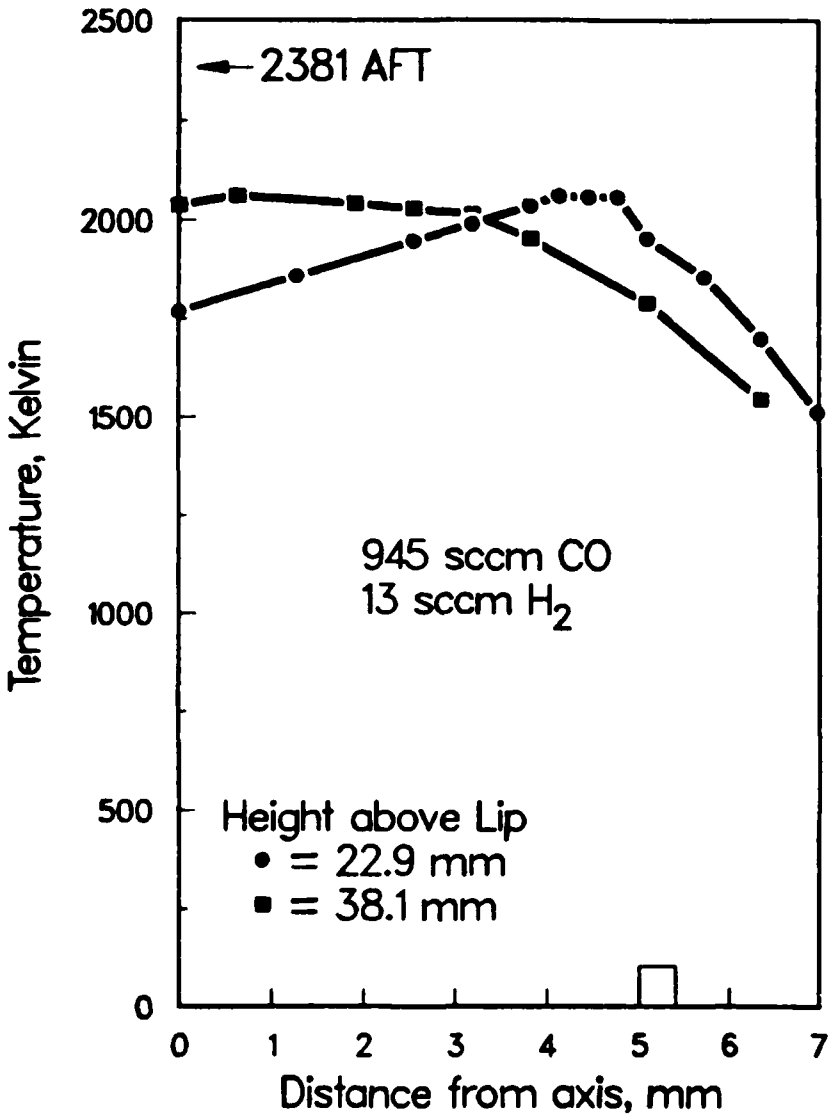

FIGURE 8 Radial temperature profiles in undiluted (CO + H_2) - air diffusion flame. Flowrate of CO was 15.8 std. cm^3/sec (945 sccm) and hydrogen, 0.2 std. cm^3/sec (13 sccm). Air flowrate was 2.1 std. ℓ/sec. Velocity ratio of air to fuel at room temperature for these conditions was 1.2. Visible tip height of flame was about 75 mm.

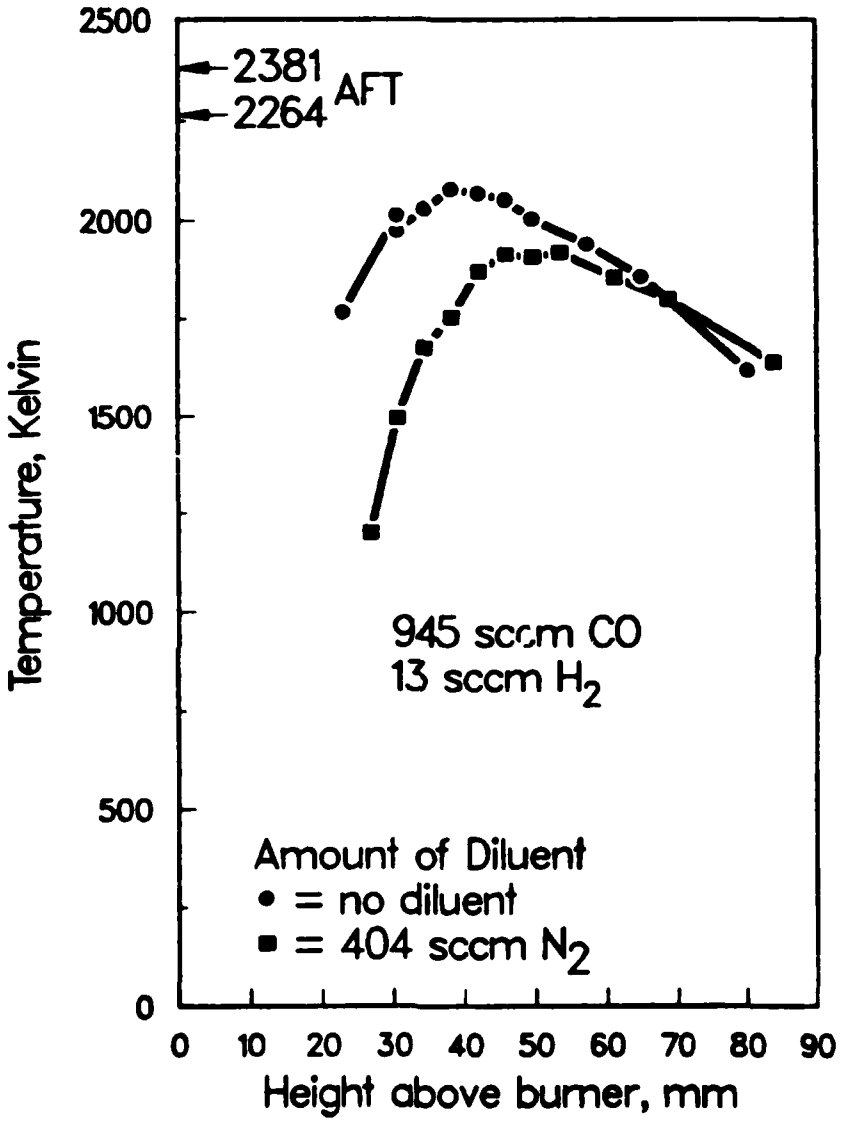

FIGURE 9 Axial temperature profiles in undiluted and nitrogen-diluted (CO + H_2)-Air diffusion flames.

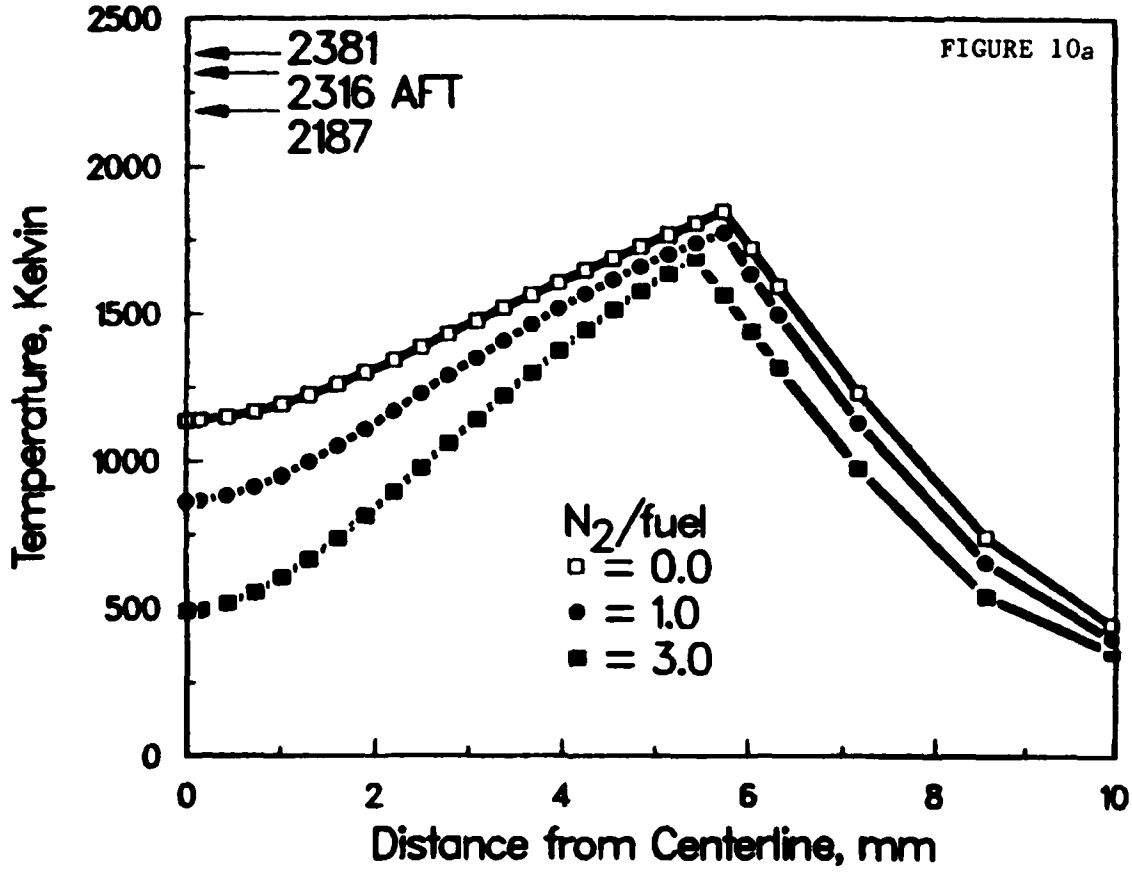

FIGURE 10 Calculated radial temperature profiles in ethylene-air diffusion flames, showing effect of nitrogen dilution. Ethylene flowrate, $\dot{V}_f$ = 3.4 std. cm^3/sec. Profiles in Figure 10a are for height z = 16.3 mm above burner and in Figure 10b for z = 38.3 mm.

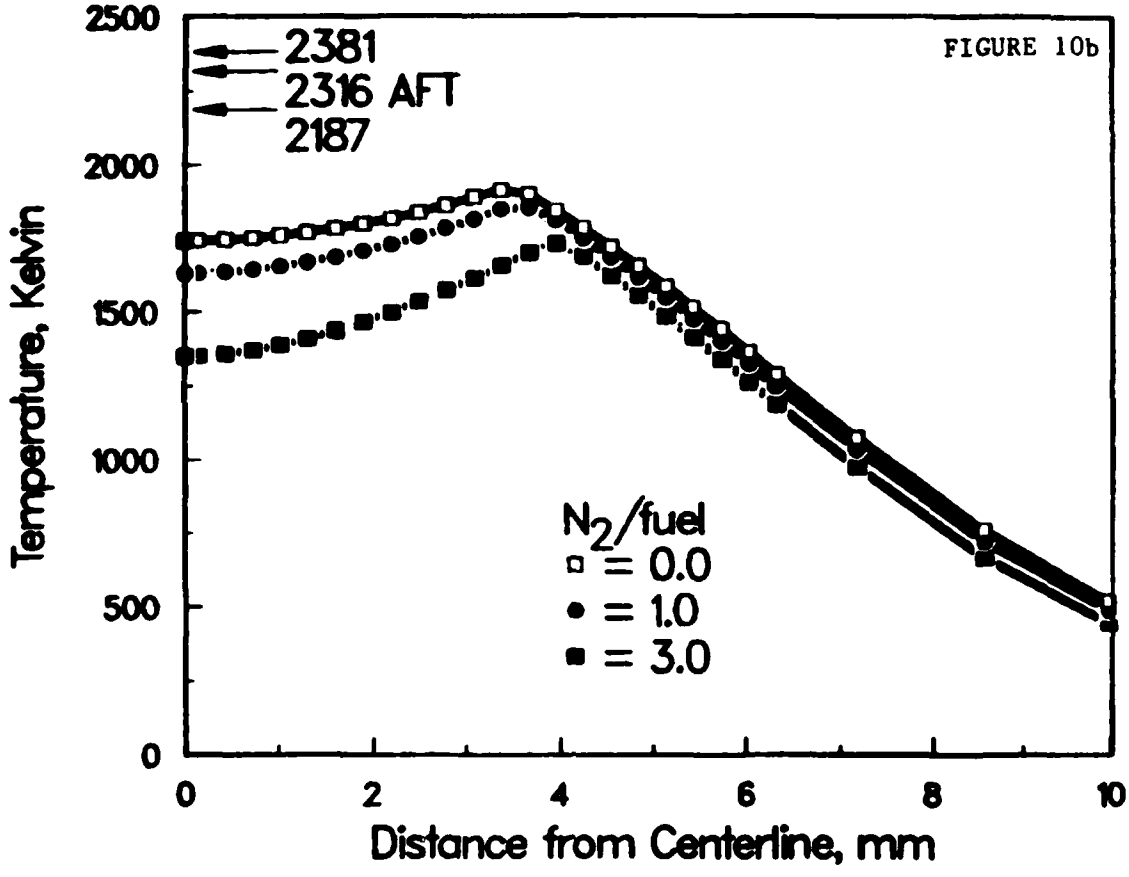
2500
2000
1500
1000
500
0
2381
2316 AFT
2187
Temperature, Kelvin
N_2/fuel
□ = 0.0
● = 1.0
■ = 3.0
0
2
4
6
8
10
Distance from Centerline, mm

FIGURE 10b

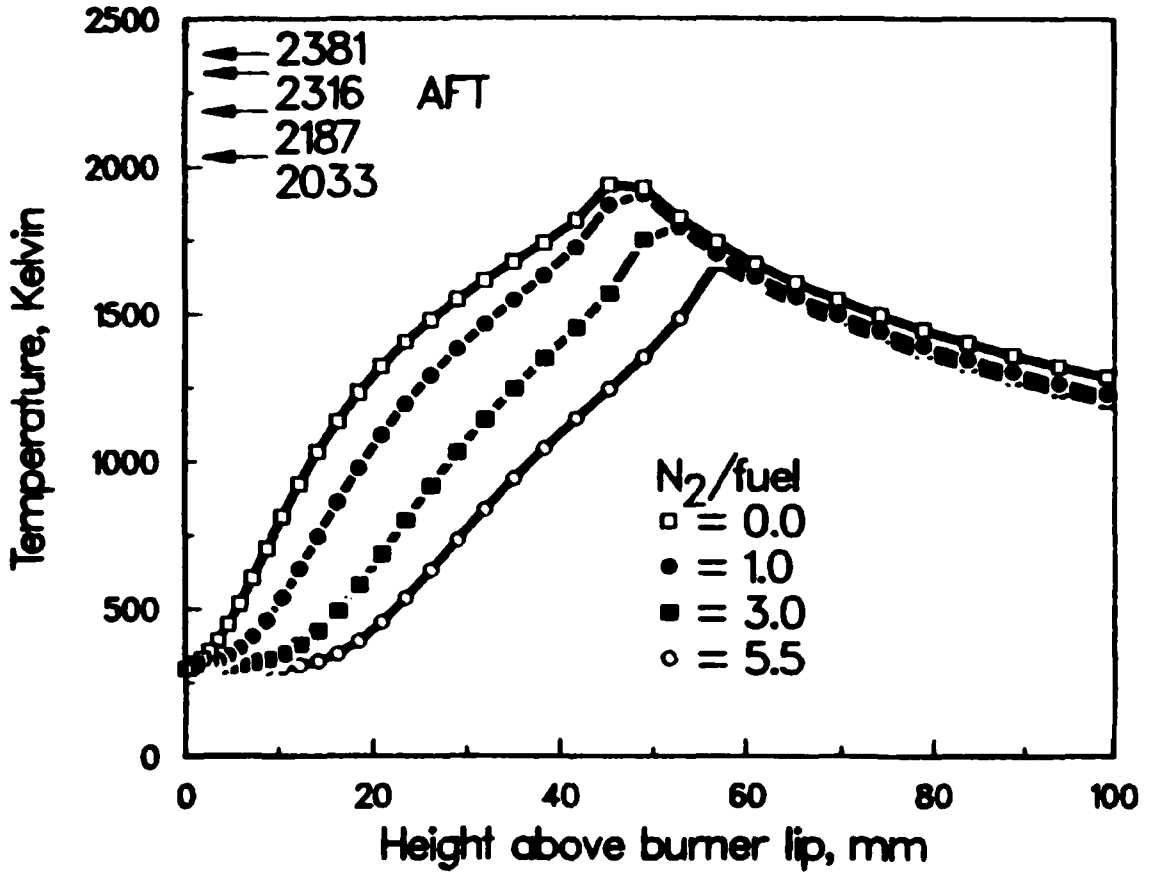

FIGURE 11 Calculated axial temperature profiles in ethylene-air diffusion flames, showing effect of nitrogen dilution. Ethylene flowrate $\dot{V}_f$ = 3.4 std. cm^3/sec.

ENCLOSURE NUMBER 1
CONTRACT DATA REQUIREMENTS LIST
INSTRUCTIONS FOR DISTRIBUTION

Addressee	DODAAD Code	Number of Copies Unclassified/Unlimited
Scientific Officer	N00014	1
Administrative Contracting Officer	FY1725	1
Director, Naval Research Laboratory, Attn: Code 2627 Washington, D.C. 20375	N00173	6
Defense Technical Information Center Bldg. 5, Cameron Station Alexandria, Virginia 22314	S47031	12
Office of Naval Research Eastern/ Central Regional Office 666 Summer Street Boston, Massachusetts 02210	N62879	1

END

FILMED

1-85

DTIC